Revisiting Properties of Ferroelectric and Multiferroic Thin Films under Tensile Strain from First Principles

Yurong Yang, Wei Ren, Massimiliano Stengel, X. H. Yan, and L. Bellaiche

Phys. Rev. Lett. **109**, 057602 — Published 2 August 2012

DOI: 10.1103/PhysRevLett.109.057602

Revisiting properties of ferroelectric and multiferroic thin films under tensile strain from first principles

Yurong Yang,[1,2] Wei Ren,[1,3] Massimiliano Stengel,[4,5] X. H. Yan,[2,6] and L. Bellaiche[1,*]

[1]*Physics Department and Institute for Nanoscience and Engineering, University of Arkansas, Fayetteville, Arkansas 72701, USA*

[2] *Physics Department, Nanjing University of Aeronautics and Astronautics, Nanjing 210016, China*

[3]*Department of Physics, Shanghai University, 99 Shangda Road, Shanghai 200444, China*

[4]*Institut de Ciència de Materials de Barcelona (ICMAB-CSIC), Campus UAB, 08193 Bellaterra, Spain*

[5]*ICREA - Institució Catalana de Recerca i Estudis Avançats, ES-08010 Barcelona, Spain*

[6] *College of Electronic Science and Engeering, Nanjing University of Posts and Telecommunication, Nanjing 210003,China*

Abstract

First-principles calculations are performed to revisit properties of (001) epitaxial $BiFeO_3$ (BFO) and $PbTiO_3$ thin films under tensile strain. While these two films possess different ground states when experiencing no misfit strain, they both exhibit the same, previously unknown phase for tensile strains above $\simeq 5\%$ at T=0K. This novel state is of orthorhombic $Pmc2_1$ symmetry, and is macroscopically characterized by a large in-plane polarization coexisting with oxygen octahedra tilting in-phase about the out-of-plane direction. On a microscopic point of view, this $Pmc2_1$ state exhibits short atomic bonds and zig-zag cation displacement patterns, unlike conventional ferroelectric phases and typical domains. Such unusual inhomogeneous patterns originate from the coexistence of polar and antiferroelectric distortions having the same magnitude, and lead BFO films to be the first known material for which orbital ordering coexists with a large polarization. Furthermore, this $Pmc2_1$ state is also found in other perovskite films under tensile strain, which emphasizes its generality.

*Electronic address: laurent@uark.edu

Epitaxial multiferroic $BiFeO_3$ (BFO) thin films constitute one of the most intensively studied materials, mainly because they exhibit several exciting phenomena when varying the misfit strain arising from the substrate on top of which the film is grown. Examples include transitions towards states with giant axial ratio and polarization [1, 2], the enhancement of magnetoelectric coefficients near these transitions [3, 4], a novel photoelectric effect [5, 6], an unusual evolution of critical temperatures with misfit strain [7], a pure gyrotropic phase transition leading to interpenetrated arrays of vortices and antivortices [8], and the nearly simultaneous occurrence of a ferroelectric and a magnetic transition near room temperature [9, 10].

Based on these recent findings, it is natural to wonder if other surprises are still in store in BFO thin films. Motivated by such a perspective, we investigated (001)-oriented BFO thin films under tensile strain (note that tensile strains are much less studied and understood in BFO, in particular [11], and in ferroelectrics, in general, than compressive strains). Interestingly, we found a previously unknown and overlooked state possessing striking atypical features for intermediate tensile strain. This state is of orthorhombic $Pmc2_1$ symmetry, and is the first known phase (to the best of our knowledge) exhibiting orbital ordering (between the d_{xz} and d_{yz} wavefunctions of the Fe ions) coexisting with a large electric polarization. Such coexistence originates from a peculiar, inhomogeneous, zig-zag-like, in-plane displacement patterns of the cations, that arise from the superposition of polar and antiferroelectric distortions – with these two different distortions having the same magnitude. This state also possesses oxygen octahedra tilting in-phase about the out-of-plane direction, in addition to these cooperative polar and antiferroelectric displacements. Moreover, to our great surprise, we also found that this $Pmc2_1$ state also emerges in the tensile region of another prototypical ferroelectric, namely $PbTiO_3$ (while BFO and $PbTiO_3$ bulks have very different ground states). As a result, this intriguing state should always be considered when investigating ferroelectric and multiferroic thin films under tensile strain, unlike what has been done so far. Note that such consideration has to be made, especially when realizing that novel phases and transitions are typically associated with new phenomena and/or enhancement of physical properties [3, 4, 8].

Density-functional calculations within the local spin density approximation (LSDA) plus the Hubbard parameter U (with U=3.8 eV for Fe ions [12, 13]) are performed, using the Vienna ab-initio simulation package (VASP) [14]. Two different (001) *epitaxial* films are

considered: those made of pure $BiFeO_3$ (BFO) and those formed by pure $PbTiO_3$ (PTO). The in-plane lattice vectors used to model these systems are: $\mathbf{a_1} = 2a_{\rm IP}\mathbf{x}$, $\mathbf{a_2} = 2a_{\rm IP}\mathbf{y}$, and $\mathbf{a_3} = a_{\rm IP}(\delta_1\mathbf{x} + \delta_\mathbf{2}\mathbf{y} + (\mathbf{2} + \delta_\mathbf{3})\mathbf{z})$, where $a_{\rm IP}$ is the in-plane lattice constant and where $\mathbf{x}$, $\mathbf{y}$ and $\mathbf{z}$ are unit vectors along the x- and y- and z-axis, respectively (these are chosen to lie along the pseudo-cubic [100], [010] and [001] directions). The supercells used to study BFO and PTO therefore contain 40 atoms, and are periodic along the $\mathbf{a_1}$, $\mathbf{a_2}$ and $\mathbf{a_3}$ axes. For a given $a_{\rm IP}$, the δ_1, δ_2 and δ_3 variables and the atomic positions are relaxed to minimize the total energy; at the variational minimum, Hellman-Feynman forces and the σ_3, σ_4 and σ_5 components of the stress tensor will vanish, thus mimicking perfect (001) epitaxy. The axial ratio of the resulting structure is provided by $1 + \frac{\delta_3}{2}$. Technically, we use the projector augmented wave method and an energy cutoff of 550 eV. A 3×3×3 k-point mesh is used for both BFO and PTO. Fe ions that are nearest neighbors of each other are imposed to have opposite magnetic moments in the studied BFO system – as consistent with the G-type antiferromagnetic order known to occur in BFO films [15]. The space groups of the different equilibrium structures found in the present study are determined by means of the "FINDSYM" and "BPLOT" programs [16]. The total polarization of each simulated material is calculated from the Bloch representation of the modern (Berry-phase) theory of polarization [17].

We numerically found that the in-plane lattice constant minimizing the total energy (to be denoted by a_{eq} in the following), is equal to 3.90 Å and 3.87 Å for BFO and PTO, respectively [18]. The misfit strain experienced by these two systems during the calculations is then defined as $\eta_{mis} = \frac{a_{\rm IP} - a_{eq}}{a_{eq}}$.

Figures 1(a) and (b) display the total energy of several structural states of low energy, as well as the axial ratio of the resulting phase possessing the lowest energy, as functions of *positive* η_{mis} (i.e., for *tensile* strain) in films made of BFO and PTO, respectively. Practically, η_{mis} is allowed to vary between 0% and $\simeq +10\%$. Figures 2 display the Cartesian components of the polarization and of the antiphase antiferrodistortive (AAFD) vector as a function of η_{mis} in these states. The AAFD vector is defined such as its axis provides the direction about which oxygen octahedra tilt in antiphase fashion, while its magnitude provides the angle of such tilting [19].

Let us first concentrate on (001) BFO films. As consistent with previous theoretical works [11, 20], these films are predicted to adopt a monoclinic Cc state for small tensile strain.

This Cc state possesses a polarization lying along a $[uuv]$ direction (with u being different from v) and oxygen octahedra tilting in antiphase fashion about a $[u'u'v']$ direction (with u' and v' differing from each other). Both the polarization and the AAFD vector rotate from the [111] to the in-plane [110] directions as η_{mis} increases within the Cc state, and are accompanied by a large decrease of the axial ratio (which is smaller than 1). The tilt associated with the AAFD vector is rather large in this phase, e.g. it is around 14 degrees for zero misfit strain. As consistent with Ref. [11], the energy of the Cc state becomes higher than the energy of an orthorhombic $Ima2$ phase for tensile strain of the order +8%. However, a previously unreported $Pmc2_1$ state is found here to be of even lower energy than both the Cc and $Ima2$ phases for $\eta_{mis} > 5.2$ % – which indicates that it can be the ground state of BFO films for moderate tensile strain, with the Cc-to-$Pmc2_1$ transition being of first-order type. This $Pmc2_1$ state is of orthorhombic symmetry and is macroscopically characterized by (1) a large in-plane polarization, oriented along the [110] direction; (2) a vanishing AAFD vector and a null z-component of the polarization; and (3) the activation of oxygen octahedra tilting *in phase* about the z-axis. The resulting in-phase tilting angle, θ_z, has a rather large magnitude (of the order of 6 degrees) near the Cc-to-$Pmc2_1$ transition, and further increases in magnitude with the tensile strain (see the inset of Fig. 2d).

Furthermore, the novel $Pmc2_1$ state in BFO films also possesses other striking characteristics. For instance, we numerically found (not shown here) that the out-of-plane component of the dielectric response in this $Pmc2_1$ state dramatically increases from 54 to 1042, when decreasing the misfit strain from +9.1% to +3.1% (which is a strain for which this phase is metastable). Moreover and as revealed by Fig. 3(a), the Bi atoms and Fe ions move in a "zig-zag" fashion: first along the in-plane [100] pseudo-cubic direction and then along the *perpendicular* but still in-plane [010] direction when going from any 5-atom unit cell to its adjacent cell along the x- or y-axis (in other words, the [100] and [010] cation displacements arrange themselves in a checkerboard pattern). These Bi and Fe displacements from their ideal positions are rather large, which result in a large (> 1.1 C/m^2) in-plane macroscopic polarization lying along the [110] direction and in nearly five-fold coordinated Fe atoms. As indicated in Fig. 3 (b), these inhomogeneous displacements can be considered as arising from a *superposition* of homogeneous atomic displacements along the [110] direction with antiferroelectric displacements – these latter having the same magnitude than the homogeneous displacements. For these antiferroelectric motions, Bi (respectively, Fe) atoms are

displaced from the $[1\bar{1}0]$ to opposite $[\bar{1}10]$ direction when going from one Bi (respectively Fe) ion to its first-nearest-neighbor Bi (respectively, Fe) ion along the x- or y-direction. Such superposition therefore involves the distortions denoted by P_{110} and $A_{\bar{1}10}$ in Ref. [21], with these two distortions being of the same magnitude here. As indicated by Fig. 2(e), these unusual atomic patterns lead to the existence of very short Fe-O bonds ($\simeq$ 1.8 Å) and long Fe-O distances ($\geq$ 2.6 Å), that are reminiscent of features found in the tetragonal-like and giant-axial -ratio phase of BFO occurring at large *compressive* strains [2, 20, 22].

Interestingly, the partial density of states shown in Figure 3(c) demonstrates that the zig-zag (or checkerboard) cation displacements induce *orbital ordering* in the Fe ions belonging to a given (001) layer: the Fe ions moving along [100] have an occupied d_{yz} orbital for energies being $\simeq$ 5.86 eV below the Fermi level while the Fe ions moving along [010] have an occupied d_{xz} orbital for this energy range. Figure 3(d) further reveals that this ordering is of C-type between the Fe layers (i.e., Fe ions on top of each other along the [001] direction have the same occupied orbital because they move along the same [100] or [010] direction). A C-type orbital ordering (coexisting with a G-type magnetic order) is known to occur in some magnetic systems [23–25] but this typically involves breathing of oxygen octahedra rather than cation motions as found here. As a result, orbital ordering does not usually coexist with a polarization. In a few recent cases, however, orbital ordering and an electrical polarization have been shown to simultaneously occur, but, for such few cases, the electric polarization is rather weak (below 0.01 C/m^2) because it is induced by the orbital or magnetic ordering [26–28]. It thus appears that the $Pmc2_1$ state of BFO is the first reported example of a state possessing orbital ordering and large polarization ($>$ 1.1 C/m^2) – as a result of large and inhomogeneous displacements of the cations.

In order to check how general is the appearance of this unusual $Pmc2_1$ state in the tensile region of epitaxial ferroelectrics and multiferroics, we now turn our attention to (001) PTO films. Figures 1(b) and 2 indicate that (001) epitaxial PTO films adopt three different ground states, depending on the value of the tensile misift strain [29]. These phases are: (1) a tetragonal P4mm state, that only exhibits a polarization along the [001] growth direction, for η_{mis} ranging between 0 and 1.2%; (2) an orthorhombic Ima2 state, for which a polarization lying along the [110] direction coexists with oxygen octahedra slightly tilting (by less than 2 degrees) in antiphase about that same in-plane direction, for η_{mis} ranging between 1.2% and 5.3% and (3) a $Pmc2_1$ state that possesses the same macroscopic structural properties

(i.e., a polarization along [110] and an in-phase oxygen octahedra tilting about [001]), short B-O bonds $\simeq 1.8$ Å and long B-O distances ≥ 2.4 Å (see Fig. 2f) as the aforementioned $Pmc2_1$ state of BFO (note that this $Pmc2_1$ state occurring at intermediate tensile strain has never been reported before in epitaxial $PbTiO_3$ films to the best of our knowledge, unlike the $P4mm$ and $Ima2$ phases [21, 30]). Interestingly, we also found (not shown here) that this $Pmc2_1$ phase also exhibits the same inhomogenuous "zig-zag" pattern of cation displacements than the one depicted in Fig. 3(a) for BFO films.

It thus appears that this inhomogeneous, intriguing $Pmc2_1$ state may be a general feature of ferroelectric and multiferroic thin films under tensile strain, and should always be considered when investigating phase diagrams of such films. Such fact is emphasized by a recent finding [21] that the ground state of $PbTiO_3/PbZrO_3$ short superlattices is indeed of $Pmc2_1$ symmetry for tensile strains larger than $\simeq 4\%$. Note, however, that the authors of Ref. [21] indicated that their $Pmc2_1$ state can only exist in *superlattices* because of the breaking of some translational symmetries with respect to pure systems, while our simulations show that such $Pmc2_1$ state also exists in pure BFO and PTO compounds. This seemingly contradictory fact can be resolved by realizing that the oxygen octahedra tilting about [001] found in Ref. [21] is in *anti-phase* fashion while it is *in-phase* in our discovered $Pmc2_1$ states of BFO and PTO films. In fact, if we start our first-principles calculations with a $Pmc2_1$ state having anti-phase tiltings in pure BFO and PTO, this structure will revert to the $Pmc2_1$ phase described in Figures 2 and 3 and that possesses in-phase tilting.

It is also important to realize that, while our predicted $Pmc2_1$ phase becomes the ground state for tensile strain of the order of +5% at T=0K in BFO and PTO films, it will likely occur at much smaller strain at finite temperature in these two films – because of the typical shape of the temperature-versus-misfit strain diagrams (see, e.g., References [31–33] and references therein). For instance, it is worthwhile to notice that an orthorhombic phase possessing a polarization along [110] and oxygen octahedra tilting (as the presently discovered $Pmc2_1$ state) was found to occur at around +4.5% at 0K but only at +2% at a temperature of 900 K in another system [33]. This is particularly promising for the experimental observation of the $Pmc2_1$ phase in BFO at finite temperature, when recalling that the Curie temperature of BFO bulk is around 1100K [34, 35]. It is also worthwhile to realize that BFO films under an epitaxial strain as large as 6% have been successively grown in the *compressive* region [1]. This large strain value is highly unusual, and is due to the fact that

BFO possesses very strong, competing degrees of freedom (polarization, antiferroelectricity, oxygen octahedra tiltings) that respond differently to strain (as consistent with our Figure 2). In other words, changing the strain affects this competition and allows BFO to transform into a different polymorphism that has the natural characteristics to adapt itself to a larger-than-usual misfit strain. Such feature strongly suggests that the $Pmc2_1$ phase of BFO may be experimentally observed even at a tensile strain of +5%. Moreover, this $Pmc2_1$ state can also become the ground state of *other* films under tensile strain. For instance, this novel phase is predicted (via 0K first-principles calculations not shown here) to occur in epitaxial perovskite $BaMnO_3$, $EuTiO_3$, and $CaTiO_3$ films for misfit strains equal or larger than 6.5%, 6.5% and 4.8% respectively – which corresponds to in-plane lattice constants of 4.12, 4.12 and 3.97 Å, respectively. Interestingly, this latter relatively small lattice constant suggests that growing $CaTiO_3$ films on $NdScO_3$ or $PrScO_3$ substrates (which are commercially available) may also render possible the experimental observation of the presently discovered $Pmc2_1$ phase.

Furthermore, this $Pmc2_1$ phase dramatically contrasts with the two kinds of ferroelectric structures typically found in the literature, that are *homogeneous* polarized phases *versus* domains in which *large* regions of space possess similar dipoles (with the dipoles belonging to different regions of space forming some angle between them) that are separated by domain walls with significant thickness. Here, the inhomogeneous displacements inherent to $Pmc2_1$ can be rather thought as *forming 90 degrees domains with no domain walls and with a single A (or B) atom belonging to each domain* [36]. It will also be interesting to determine how the unusual characterisistics of the $Pmc2_1$ phase evolve with temperature. A well-used numerical tool that typically allows such investigation is the so-called first-principles-based effective Hamiltonian [37]. However, one particular assumption of such Hamiltonian is that the dipoles are either centered on A or the B-site of the ABO_3 perovskite structure. Interestingly, centering such dipoles on A (respectively, B) sites prevents the possibility of inhomogeneous displacements at the B (respectively, A) sites to form within the usual effective Hamiltonian scheme, which is problematic to the study of the $Pmc2_1$ state since Figs. 3 reveal that *both* A and B sites have inhomogenous displacements in that peculiar phase. In other words, the present discovery of this $Pmc2_1$ phase also calls for the development of new finite-temperature tools!

We therefore hope that the present work is of large benefits to the active research fields of

phase transitions, nanoscience, ferroelectrics, magnets and multiferroics, since it, e.g., points out the existence of a novel phase that is associated with unusual inhomogeneous atomic displacements in thin films made of two prototypical multiferroics and ferroelectrics and the occurrence of a large polarization within an orbitally-ordered state.

This work is mostly supported by the Department of Energy, Office of Basic Energy Sciences, under contract ER-46612. We also acknowledge NSF grants DMR-1066158 and DMR-0701558, ARO Grant W911NF-12-1-0085 and ONR Grants N00014-11-1-0384 and N00014-08-1-0915. M. S. acknowledges support by DGI-Spain through Grants No. MAT2010-18113 and No. CSD2007-00041, and by the European Union through the project EC-FP7, Grant No. NMP3-SL-2009-228989 "OxIDes". Some computations were also made possible thanks to the MRI grant 0722625 from NSF, the ONR grant N00014-07-1-0825 (DURIP) and a Challenge grant from the Department of Defense.

[1] R. J. Zeches, M. D. Rossell, J. X. Zhang, *et al.*, *Science* **326**, 977 (2009).

[2] H. Béa, B. Dupé, S. Fusil, *et al.*, *Phys. Rev. Lett.* **102**, 217603 (2009).

[3] J. C. Wojdeł and J. Íñiguez, *Phys. Rev. Lett.* **105**, 037208 (2010).

[4] S. Prosandeev, I. A. Kornev, and L. Bellaiche, *Phys. Rev. B* **83**, 020102 (2011).

[5] S. Y. Yang, J. Seidel, S. J. Byrnes, *et al.*, *Nature Nanotech.* **5**, 143 (2010).

[6] J. Seidel, D. Fu, S.-Y. Yang, *et al.*, *Phys. Rev. Lett.* **107**, 126805 (2011).

[7] I. C. Infante, S. Lisenkov, B. Dupé, *et al.*, *Phys. Rev. Lett.* **105**, 057601 (2010).

[8] S. Prosandeev, I. A. Kornev, and L. Bellaiche, *Phys. Rev. Lett.* **107**, 117602 (2011).

[9] I. C. Infante, J. Juraszek, S. Fusil, *et al.*, *Phys. Rev. Lett.* **107**, 237601 (2011).

[10] K.-T. Ko, M. H. Jung, Q. He, *et al.*, *Nature Commun.* **2**, 567 (2011).

[11] B. Dupé, S. Prosandeev, G. Geneste, *et al.*, *Phys. Rev. Lett.* **106**, 237601 (2011).

[12] I. A. Vladimir, F. Aryasetiawan, and A. I. Lichtenstein, *J. Phys: Condens. Matter* **9**, 767 (1997).

[13] I. A. Kornev, S. Lisenkov, R. Haumont, *et al.*, *Phys. Rev. Lett.* **99**, 227602 (2007).

[14] G. Kresse and D. Joubert, *Phys. Rev. B* **59**, 1758 (1999).

[15] H. Béa, M. Bibes, A. Barthélémy, *et al.*, *Appl. Phys. Lett.* **87**, 072508 (2005).

[16] See http://www.cryst.ehu.es/cryst/bplot.html. And see http://stokes.byu.edu/findsym.html.

[17] R. D. King-Smith and D. Vanderbilt, *Phys. Rev. B* **47**, 1651 (1993).

[18] Note that our theoretical lattice constants are underestimated by roughly 1-2% with respect to measurements due to the use of the LSDA scheme.

[19] A. Glazer, *Acta Crystallogr., Sect. B* **28**, 3384 (1972).

[20] A. J. Hatt, N. A. Spaldin, and C. Ederer, *Phys. Rev. B* **81**, 054109 (2010).

[21] J. L. Blok, D. H. A. Blank, G. Rijnders, *et al.*, *Phys. Rev. B* **84**, 205413 (2011).

[22] B. Dupé, I. C. Infante, G. Geneste, *et al.*, *Phys. Rev. B* **81**, 144128 (2010).

[23] G. R. Blake, T. T. M. Palstra, Y. Ren, *et al.*, *Phys. Rev. B* **65**, 174112 (2002).

[24] Y. Tokura and N. Nagaosa, *Science* **288**, 462 (2000).

[25] S.-W. Cheong, *Nature Mater.* **6**, 927 (2007).

[26] J. Okamoto, D. J. Huang, C. Y. Mou, *et al.*, *Phys. Rev. Lett.* **98**, 157202 (2007).

[27] P. Barone, K. Yamauchi, and S. Picozzi, *Phys. Rev. Lett.* **106**, 077201 (2011).

[28] A. Stroppa, P. Jain, P. Barone, *et al.*, *Angew. Chem. Int. Edit.* **50**, 5847 (2011).

[29] Note that we also found Cm and Cc states that are very close in energy to the $P4mm$ and $Ima2$ phases for a tensile strain close to +1% in PTO films.

[30] C. Bungaro and K. M. Rabe, *Phys. Rev. B* **69**, 184101 (2004).

[31] N.A. Pertsev, A.G. Zembilgotov and A.K. Tagantsev, *Phys. Rev. Lett.* **80**, 1988 (1998).

[32] B.-K. Lai, I.A. Kornev, L. Bellaiche and G.J. Salamo, *Appl. Phys. Lett* **86**, 132904 (2005).

[33] D. Sichuga, I. Ponomareva and L. Bellaiche, *Phys. Rev. B* **80**, 134116 (2009).

[34] J.R. Teague, R. Gerson and W.J. James, *Solid State Comm.* **8**, 1073 (1970).

[35] S.V. Kiselev *et al*, *Sov. Phys. Dokl.* **7**, 742 (1963); G.A. Smolenskii *et al*, *Sov. Phys. Solid State* **2**, 2651 (1961).

[36] Note that preliminary results indicate that these unusual zig-zag patterns mostly originate from a subtle coupling energy involving the product of the square of the displacements of the A atoms along the x- (or y-) axis with the in-phase tilting about the z-axis.

[37] W. Zhong, D. Vanderbilt, and K. M. Rabe, *Phys. Rev. B* **52**, 6301 (1995).

FIG. 1: (Color online) Predicted total energy (left vertical axis) and axial ratio (right vertical axis) versus the tensile misfit strain for low-in-energy phases in epitaxial (001) BFO films (Panel a), and PTO films(Panel b).

FIG. 2: (Color online) Predicted physical properties of epitaxial (001) BFO and PTO films versus tensile misfit strain in the equilibrium phases. Panels (a) and (b) show the x-component (which is identical to its y-component) and the z-component of the total polarization, respectively. Panels (c) and (d) display the x-component (which is identical to its y-component) and the z-component of the AAFD vector (see text), respectively. The inset of Panel (d) represents the angle made by oxygen octahedra tilting *in-phase* about the z-axis, θ_z. Panels (e) and (f) show the nearest neighbor Fe-O lengths and Ti-O lengths in BFO and PTO films, respectively.

FIG. 3: (Color online) Features of the $Pmc2_1$ state of BFO. Panel (a) displays atomic characteristics, and emphasizes the inhomogenous in-plane displacements of the cations. Panel (b) schematizes these displacements in terms of the sum of a polar and antiferroelectric distortion. Panel (c) shows the partial density of states related to the d_{xy}, d_{yz} and d_{xz} orbitals of two Fe ions belonging to the same (001) layer. Panel (d) shows the C-type ordering between the d_{yz} and d_{xz} orbitals of Fe ions in the BFO films. In Panel (b), the Bi (respectively, Fe) atoms are indicated by filled (respectively, open) circles, and the Bi and Fe atoms belong to different (001) planes.

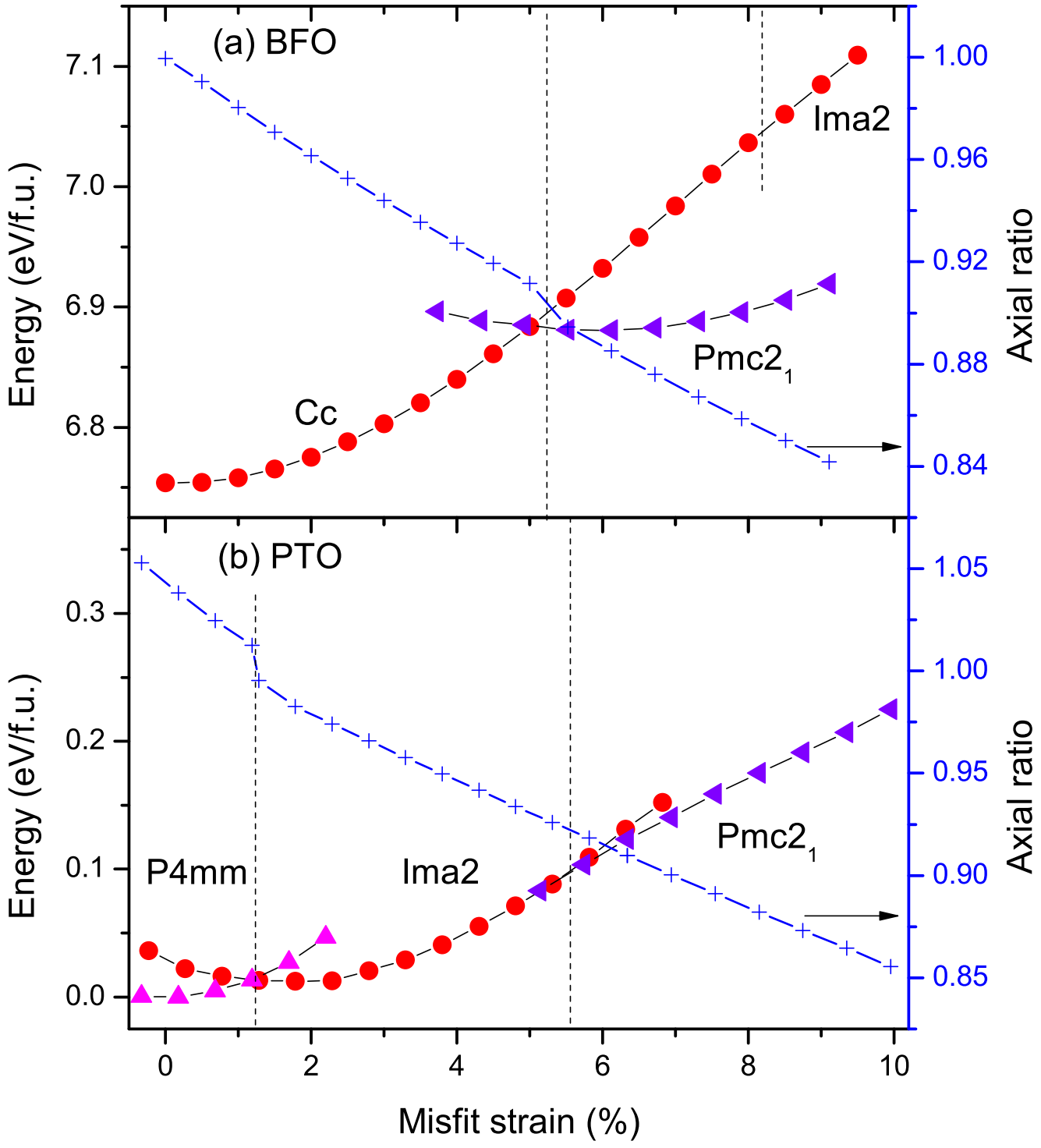

Figure 1 LP12929 25Jun2012

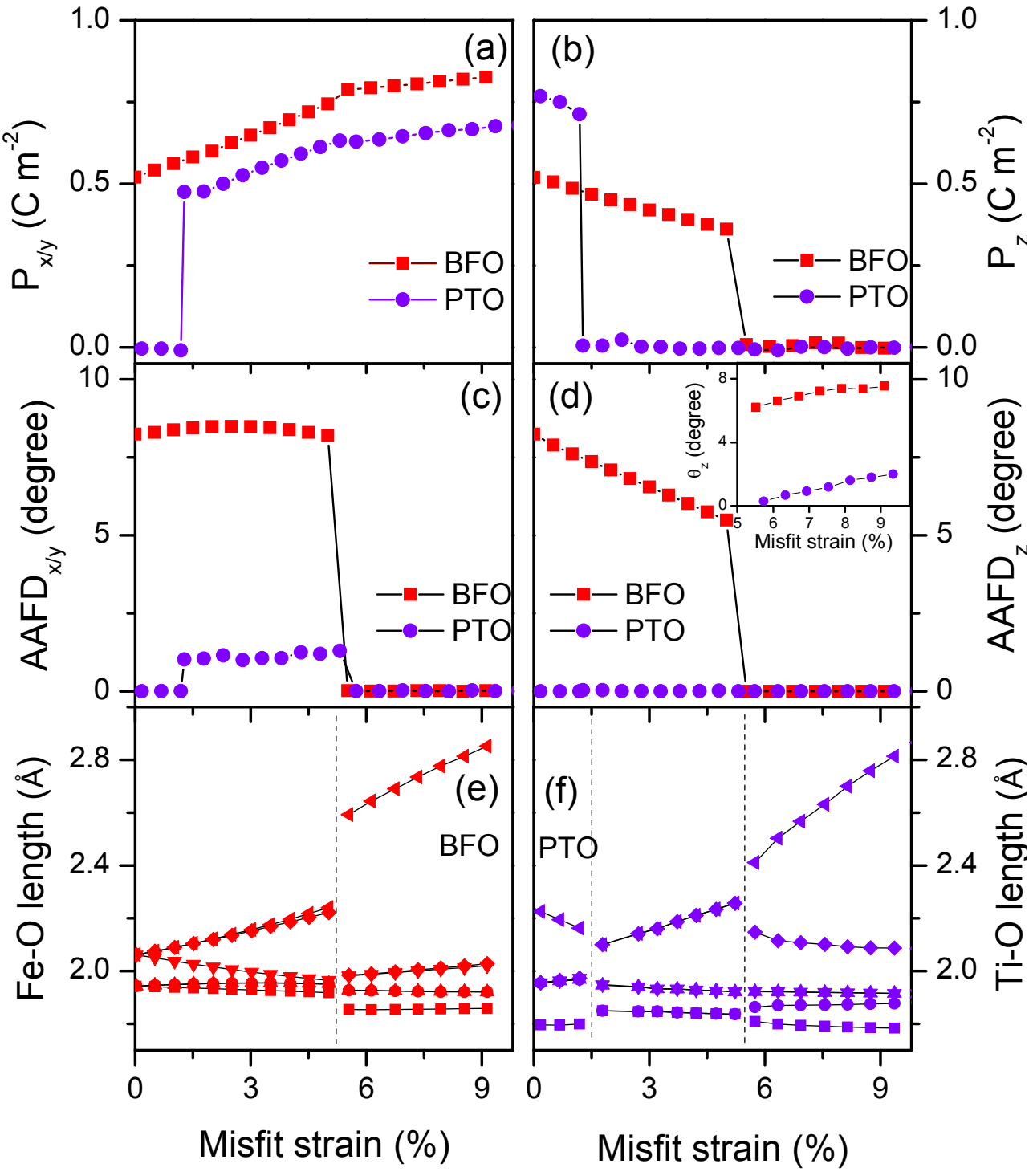

Figure 2 LP12929 25Jun2012

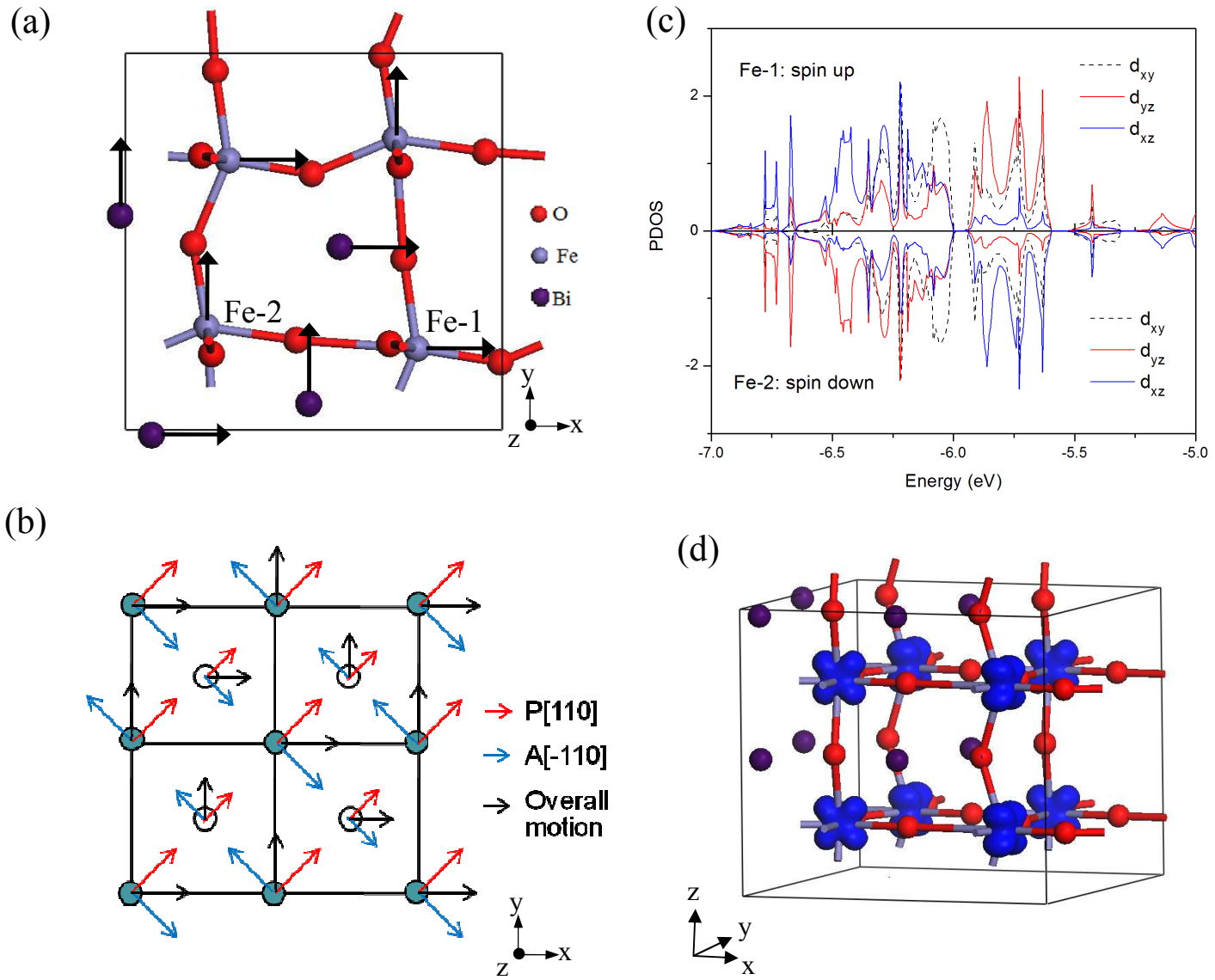

Figure 3 LP12929 25Jun2012